International Journal of Medical, Medicine and Health Sciences
ISSN: 2517-9969
Vol:11, No:12, 2017

Classification of State Transition by Using a Microwave Doppler Sensor for Wandering Detection

K. Shiba, T. Kaburagi, Y. Kurihara

***Abstract*—**With global aging, people who require care, such as people with dementia (PwD), are increasing within many developed countries. And PwDs may wander and unconsciously set foot outdoors, it may lead serious accidents, such as, traffic accidents. Here, round-the-clock monitoring by caregivers is necessary, which can be a burden for the caregivers. Therefore, an automatic wandering detection system is required when an elderly person wanders outdoors, in which case the detection system transmits a 'moving' followed by an 'absence' state. In this paper, we focus on the transition from the 'resting' to the 'absence' state, via the 'moving' state as one of the wandering transitions. To capture the transition of the three states, our method based on the hidden Markov model (HMM) is built. Using our method, the restraint where the 'resting' state and 'absence' state cannot be transmitted to each other is applied. To validate our method, we conducted the experiment with 10 subjects. Our results show that the method can classify three states with 0.92 accuracy.

***Keywords*—**Wander, microwave Doppler sensor, respiratory frequency band, the state transition, hidden Markov model.

I. Introduction

ELDERLY population has been increasing in many developed country. According to the World Health Organization (WHO), the majority of developed countries are estimated to have 1.4 billion in elderly population over 65 years old by 2030 [1]. This implies that the number of people requiring nursing care will only increase within those countries. In one study, the number of PwD has increased in recent years [2]. PwD are likely to wander and unconsciously set foot outdoors, making them susceptible to serious accidents; for example, traffic accidents [3]. Therefore, the detection of a wandering elderly is required. However, round-the-clock monitoring can be a burden to caregivers. Hence, an automatic wandering detection using sensors is required in order to provide immediate response when an elderly person wanders.

Systems based on GPS have been proposed for the detection of wandering [4], [5], for example, Solanas tries to recognize an elderly's position when he/she is wandering outside [4]. Although a GPS can detect the movement of an object outdoors, it does not perform as well while trying to detect an object in a room, or when no obstacle is present. Moreover, the response may be delayed if the elderly goes from indoors to outdoors. Here, we focus on monitoring the elderly in their homes. The moment an elderly's state changes to "absence," monitoring is required. Here, when an elderly wanders and goes outdoors, the state changes from the "resting" to "absence" state, via the "moving" state. Therefore, before the "absence" state is classified, the classification of the "moving" state is required. In wandering, the two types of state transition, "moving"-to-"absence", "absence"-to-"moving"-to-"absence" and "resting"-to-"moving"-to-"absence", are considered.

Elloumi had proposed a human activity recognition system based on a movie camera [6]. Although moving technology has shown great progress in recent years, using a movie camera is an invasion of privacy, especially when it is used in bathrooms and toilets. Therefore, the use of other devices has been considered.

Ma et al. had proposed a method to classify a human's presence/absence as well as recognizing activity using infrared pyroelectric sensors [7], [8]. Pyroelectric sensors are able to obtain an object's temperature. Therefore, using the captured temperature, a human's presence/absence can be classified. One problem with pyroelectric sensors is that response may be difficult to achieve when the atmospheric temperature changes to a value similar to that of a human's body temperature.

Okuya and Sekine had proposed a human presence/absence classification and activity recognition system based on using a microwave Doppler sensor, which can capture an object's motion [9], [10]. We have also previously used a microwave Doppler sensor to classify human presence/absence [11]. In our work [11], we were able to classify "sitting on a chair" and "absence" with 0.99 accuracy.

In this paper, we propose a system that classifies three human states: "resting", "moving," and "absence." Using data from a microwave Doppler sensor, a wandering model that can take into account the transition of the three states is developed.

II. Proposed Method

Our method is described in this section. A microwave Doppler sensor can capture a human's motion, such as respiration, walking, standing and so on. Capturing a human's characteristic motion is required to classify the three states: "resting", "moving" and "absence." Here, we propose setting a microwave on the ceiling so that a wider area can be covered. By radiating the microwave downwards, we can expect the capture of the features corresponding to each of the three states. Fig. 1 shows our method, which is separated into the learning phase (A) and the estimation phase (B). A microwave Doppler sensor outputs time-series signal $I(t)$ corresponding to an object's motion. Let t and k be continuous time and discrete time, respectively. All acquired data are first converted to digital signals, $I(k)$ with sampling interval dt. Further, let

K. Shiba is with the Department of Science and Engineering, Aoyama Gakuin University, Sagamihara, Japan (phone: +81-080-6776-3829; e-mail: sbkzaa@gmail.com).

T. Kaburagi and Y. Kurihara are with Aoyama Gakuin University, Sagamihara, Japan (e-mail: t23489@aoyamagakuin.jp, kurihara@ise.ac.aoyama.jp).

$F(=1/dt)$ be the sampling frequency within measurement. In the learning phase, the wandering model is developed using $I(k)$. In the estimation phase, the state of unknown data is estimated by the developed model.

A. Learning Phase

Initially, a certain amount of data, $I(k)$, which corresponds to a subject's state, that is, the "absence", "resting", and "moving" states, are measured as learning data sets. Here, let N be the number of measurement data (1, 2, 3, …, n,…, N). Therefore, N learning data sets, $I_n(k)$, are acquired. All $I_n(k)$ are labeled $e_n(k) \in \{1,2,3\}$ for each time step k (1: absence state, 2: resting state, 3: moving state). Here, let f be the discrete frequency. $I_n(k)$ is converted to $W_n(k,f)$ by Wavelet transform (WT) with three parameters, f_{start}, f_{end} and df. Let f_{start}, f_{end} and df be the lowest frequency, the highest frequency and the frequency resolution, respectively, in WT. $W_n(k,f)$ denotes the frequency characteristic for each time step k. Using $W_n(k,f)$, two types of feature vector, $S_n(k)$ and $R_n(k)$, are calculated. Here, the frequency band from f_{low} and f_{high} is decided. As shown in (1), the summation of amplitude between f_{start} and f_{end} is calculated for each k as $S_n(k)$. As shown (2), the ratio of $S_n(k)$ and the summation between f_{low} and f_{high} is calculated as $R_n(k)$. All $I_n(k)$ are converted into $S_n(k)$ and $R_n(k)$.

$$S_n(k) = \sum_{f=f_{low}}^{f_{high}} W(k,f) \tag{1}$$

$$R_n(k) = \sum_{f=f_{low}}^{f_{high}} W(k,f) \Big/ \sum_{f=f_{start}}^{f_{end}} W(k,f) \tag{2}$$

Using all $S_n(k)$ and $R_n(k)$, the thresholds for categorization, TS_1, TS_2, TR_1, TR_2, are calculated. First, in order to obtain the thresholds TS_1 and TS_2, CS_1, CS_2 and CS_3 are calculated from $S_n(k)$ as shown in (3)-(5).

$$CS_1 = \text{median}(S_n(k)|_{e_n(k)=1}) \tag{3}$$

$$CS_2 = \text{median}(S_n(k)|_{e_n(k)=2}) \tag{4}$$

$$CS_3 = \text{median}(S_n(k)|_{e_n(k)=3}) \tag{5}$$

$S_n(k)|_{e_n(k)=1}$ denotes a collection of $S_n(k)$ where $e_n(k)=1$.

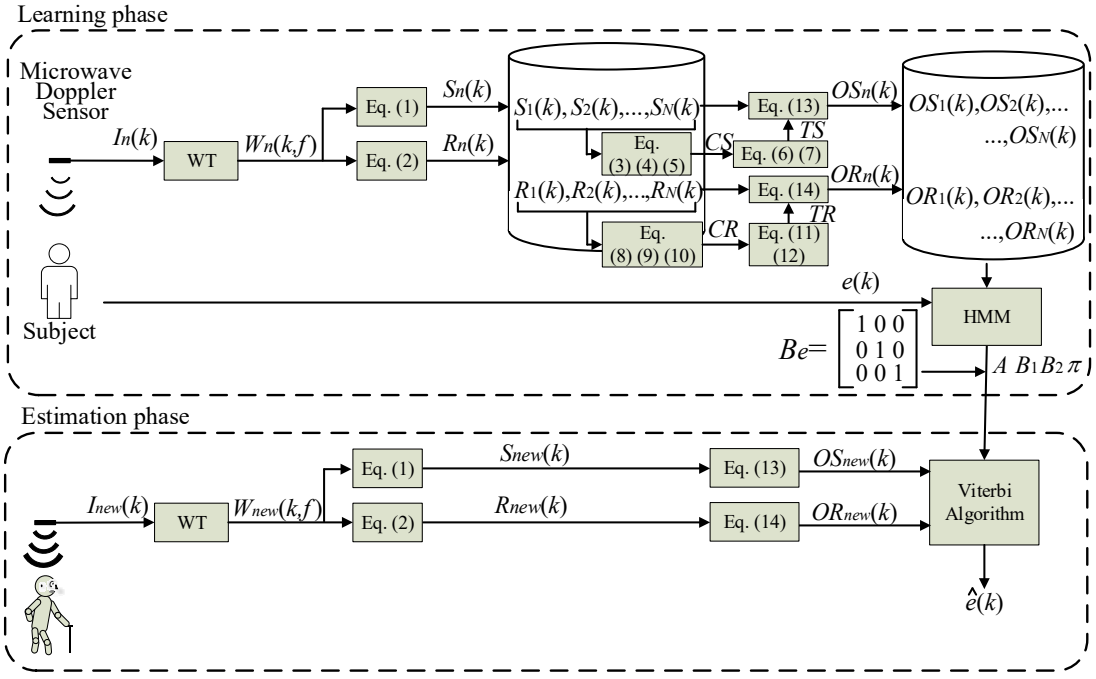

Fig. 1 Overview of the proposed method

Next, CS_1, CS_2 and CS_3 are sorted in ascending order. For example, if CS_1 is larger than CS_2, the value of CS_1 and CS_2 are exchanged. The thresholds TS_1 and TS_2 are calculated using (6) and (7):

$$TS_1 = (CS_1 + CS_2)/2 \tag{6}$$

$$TS_2 = (CS_2 + CS_3)/2 \tag{7}$$

TR_1 and TR_2 are calculated using (8)-(12) using $R_n(k)$ and $S_n(k)$.

$$CR_1 = \text{median}(R_n(k)|_{e_n(k)=1}) \tag{8}$$

$$CR_2 = \text{median}(R_n(k)|_{e_n(k)=2}) \quad (9)$$

$$CR_3 = \text{median}(R_n(k)|_{e_n(k)=3}) \quad (10)$$

$$TR_1 = (CR_1 + CR_2)/2 \quad (11)$$

$$TR_2 = (CR_2 + CR_3)/2 \quad (12)$$

Using both types of threshold, $S_n(k)$ and $R_n(k)$ are categorized to $OS_n(k)$ and $OR_n(k)$ using (13) and (14):

$$OS_n(k) = \begin{cases} 1 & : \quad S_n(k) < TS_1 \\ 2 & : \quad TS_1 \le S_n(k) < TS_2 \\ 3 & : \quad S_n(k) \ge TS_2 \end{cases} \quad (13)$$

$$OR_n(k) = \begin{cases} 1 & : \quad R_n(k) < TR_1 \\ 2 & : \quad TR_1 \le R_n(k) < TR_2 \\ 3 & : \quad R_n(k) \ge TR_2 \end{cases} \quad (14)$$

$E_1(k)$ and $E_2(k)$ are used to learn the HMM wandering model. The parameters of HMM, i.e., the state transition probabilities, the emission probabilities, and the initial state probabilities, are learned by measurement learning data. In this paper, the transition of state, $s(k) \in \{1,2,3\}$ is modeled as the state transition probabilities, $A(s(k),s(k+1))$. Here, we define that the transition between the "resting" and "absence" states cannot be performed. Hence, $A(1,2)$ and $A(2,1)$ are fixed at 0. The relation between $OS(k)$ and $s(k)$ is modeled as the emission probabilities, $B_S(s(k),OS(k))$. As well as $B_S(s(k),OS(k))$, the relation between $OR(k)$ and $s(k)$ is modeled as the emission probabilities, $B_R(s(k),OR(k))$. In addition, for the true state in learning, $e(k)$, its emission probability, $B_e(s(k),e(k))$ whose diagonal factor is defined as 1 is modeled. Let π be the initial state probabilities. Using the Baum-Welch algorithm, A, B_S, B_R and π are updated by $OS(k)$, $OR(k)$ and B_e. Updating of A, B_S, B_R and π with the Baum-Welch algorithm is repeated R times. Further, the logarithm likelihood between the updated model and the learning data, L is calculated. If L is lower than ε, updating is stopped and A, B_S, B_R and π are applied at this instance.

B. Estimation Phase

In the estimation phase, the unknown data, $I_{new}(k)$ is obtained. By using TS_1, TS_2, TR_1 and TR_2 obtained by learning data sets, $I_{new}(k)$ is converted to feature vectors, $OS_{new}(k)$ and $OR_{new}(k)$. Here, in order to obtain the optimal path, the Viterbi algorithm is utilized with A, B_S, B_R, $OS_{new}(k)$ and $OR_{new}(k)$ as shown in (15).

$$\hat{s}(k) = \text{Viterbi}(OS(k),OR(k) \mid A,B_S,B_R,\pi) \quad (15)$$

Additionally, by using (16) with the optimal path $\hat{s}(k)$, the estimation result $\hat{e}(k)$ is acquired for each k.

$$\hat{e}(k) = \arg\max_e (P(e \mid B_e, \hat{s}(k))) \quad (16)$$

III. Experiment

We conducted an experiment in order to evaluate our method.

A. Experimental Setup

Fig. 2 shows our experimental setup and the measurement system. A microwave Doppler sensor, IPS154, was set at a height of 2.3 m from the floor. The height corresponds to the height of a general ceiling and a single device can cover an area of radius 1.5 m. In this covered area, the "absence", "resting", and "moving" states were measured with a 0.01 seconds of sampling interval (*dt)* in 30 seconds. Further, we conducted the experiment with 10 healthy subjects who participated with informed consent. The age of the subjects is between 20–24 years old.

For signal processing, 0.1 Hz, 50 Hz and 0.1 Hz are set to f_{lstart}, f_{end} and df, respectively. Additionally, when calculating the feature vector, f_{low} and f_{high} were set to 0.2 Hz and 0.8 Hz, respectively. These frequencies correspond to a human's respirational frequency band. Each of the parameters: HMM, A, B, and π are, initially, set to a uniform random number based on the rand function in Matlab 2017. The repeated number, R and the threshold, ε in the Baum-Welch algorithm are set 500 and 1.00×10^{-3}, respectively.

B. Experimental Data

All three states: "moving", "resting" and "absence" are taken into account in our measurements. The "moving" and "resting" states are obtained when a subject is "walking" and "sitting," respectively. At first a subject is asked to sit on a chair calmly to initiate the "resting" state. After a few seconds, we asked the subjects to stand up and walk in the experimental area to obtain the "moving" state. Before the entire measurement time (30 seconds) has passed, the subjects are asked to leave the experimental area. The term "absence" is labeled as the duration when the subjects begin to leave until measurement is finished. Within the measurement of data $I(k)$, the true state $e(k)$ is checked and labeled for each discrete time step k. The process flow explained above is repeated 20 times for each subject. Therefore, 200 data $I(k)$ are acquired totally.

C. Evaluation

All $I(k)$ are converted into feature vector $OS(k)$ and $OR(k)$ with true state $e(k)$. We performed the evaluation based on the leave-one-subject-out-manner. One subject's $OS(k)$ and $OR(k)$ are applied as test data set, and the other subjects' $OS(k)$ and $OR(k)$ are used as learning data sets to develop, A, B_S, B_R, π (N=180).

The true state and the classified state are compared for each time step k. Table I shows nine types of classification results, where three types of correct cases and six types of incorrect cases were obtained. For the correct cases, the "resting",

"moving" and "absence" states are classified as TR, TM, and TA, respectively, as shown in Table I. However, for the incorrect cases, the "resting", "moving" and "absence" states are classified as other states, denoted by TR1 or TR2, TM1 or TM2, and TA1 or TA2, respectively. Each type of classification is as shown in Table I.

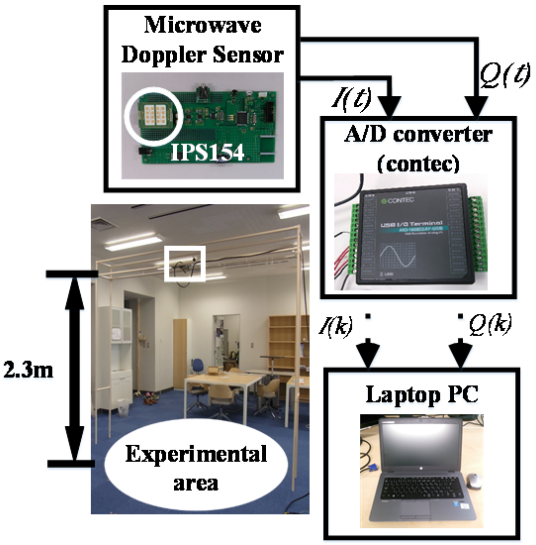

Fig. 2 Our experimental setup. The measurement data $I(t)$ is sent to an A/D converter and converted into $I(k)$

TABLE I
RESULT OF EVALUATION I

		True State		
		"Resting"	"Moving"	"Absence"
Classified State	"Resting"	*TR*	*FR*1	*FR*2
	"Moving"	*FM*1	*TM*	*FM*2
	"Absence"	*FA*1	*FA*2	*TA*

$$accuracy = \frac{TR + TM + TA}{TP + FR1 + FR2 + FM1 + TM + FM2 + FA1 + FA2 + TN} \quad (17)$$

The evaluation flow above is repeated 10 times for each subject, and each classification result is counted up using all of the subjects' data. The ratio of each index for all classification results are calculated so that the summation of all indexes represents 1. Further, using these indexes, the accuracies are calculated for each subject.

Additionally, to validate our HMM-based model, we used two types of classification methods. The first method does not use HMM and classifies only the thresholds T_S and T_R. Using $OS(k)$, the state, $\hat{e}(k)$, is estimated and accuracies are calculated. The second method is based on HMM, in which there are no restrictions to the transition of states. In the initialization of the state transition matrix A, none of the factors takes 0. Both comparison methods are also evaluated based on the leave-one-subject-out-manner. Moreover, in order to confirm how each feature vector, $S(k)$ and $R(k)$, works in this classification, each state is classified using a single feature vector. According to our previous study [11], we can classify a human's presence/absence with 0.98 accuracy by using only the summation between the amplitude of the respirational frequency band. Our previously-reported feature [11] is similar to this experiment's $S(k)$. Here, in this evaluation, we assume that, while $S(k)$ is useful to distinguish a human's absence from presence, $S(k)$ is also useful in classifying the "resting" and "moving" states. Therefore, we validated that a human's presence/absence can be classified using our HMM-based method, where only $OS(k)$ is required. Both the "moving" and "resting" states are distinguished as "present" state from "absence" state (evaluation type I). In addition, we validated that a human's "resting" and "moving" states can be classified using our HMM-based method, where only $OR(k)$ is required (evaluation type II). In both evaluation types, the accuracy of presence/absence classification and the accuracy of "resting"/"moving" classification are calculated as shown in (18) and (19):

$$accuracy_{PA} = \frac{TR + FR1 + FM1 + TM + TA}{TP + FR1 + FR2 + FM1 + TM + FM2 + FA1 + FA2 + TN} \quad (18)$$

$$accuracy_{RM} = \frac{TR + TM}{TP + FR1 + FR2 + FM1 + TM + FM2} \quad (19)$$

IV. Experimental Results

A. Examples of Measurement Data

Figs. 3-6 show examples of our measurements and signal processing. From the beginning to about 8 s, a subject sat on a chair calmly, also known as the "resting" state. Next, the subject stood up and was walking in the experimental area for 19 s, classified as the "moving" state. Finally, the subject goes outdoors at 19 s and no subjects are found in the experimental area by the end of the measurement. This scenario is measured as the "absence" state.

Fig. 3 shows an example of (a) the measurement data $I(k)$, and (b) the frequency characteristic $W(k,f)$ of this experiment. As shown Fig. 3 (a), although $I(k)$ is shaped flatly during the "resting" and "absence" states, $I(k)$ varies significantly during the "moving" state. The "resting" and "absence" states are similar in shape. Here, as shown Fig. 3 (b), the frequency shows stronger amplitudes during the "moving" state. During the "resting" state at lower frequencies, i.e. less than 2 Hz, the frequency shows stronger amplitudes than any other frequency bands. During the "absence" state, the frequencies show weaker amplitudes. However, as shown in Fig. 3 (b), stronger amplitudes occur at lower frequencies, i.e. less than 2 Hz. From 8 s to 19 s, a subject walks in the experimental area, also known as the "moving" state. During the "moving" state, $I(k)$ changed significantly. As shown in Fig. 3 (b), most of the frequencies have strong amplitudes.

Fig. 4 shows (a) the feature vector $S(k)$, and (b) the feature vector $R(k)$, obtained from the frequency characteristic, $W(k,f)$ shown in Fig. 3 (b). The values of $S(k)$ and $R(k)$ correspond to $W(k,f)$. Within the "resting" state, while $S(k)$ varies only a little, $R(k)$ varies significantly. On the other hand, within the "moving" state, while $S(k)$ varies significantly, $R(k)$ varies only a little.

While the subject is taking the "absence" state, $S(k)$ and $R(k)$ mostly vary only a little. However, at about 24 s, $R(k)$ temporarily varies significantly.

Fig. 5 shows (a) the categorized data $OS(k)$, and (b) the categorized data $OR(k)$ from Fig 4's $S(k)$ and $R(k)$. Within the "resting" state, while $S(k)$ shows 2 or 3, $R(k)$ shows mostly 3. Within the "moving" state, while $S(k)$ shows only 3, $R(k)$ shows 1 or 2 mostly, but also 3 sometimes. And, within the "absence" state, $S(k)$ and $R(k)$ show all categories: 1, 2 and 3. From 19 s to 21 s, in the first term of the "absence" state, $S(k)$ shows 3. However, in other terms of the "absence" state, $S(k)$ shows 1 or 2.

Fig. 6 shows (a) the classified state using HMM, $\hat{e}(k)$ and (b) the true state transition $e(k)$. The state transition can be captured by $\hat{e}(k)$. However, some time lags are shown at the starting point of "moving" between $\hat{e}(k)$ and $e(k)$. $\hat{e}(k)$ is delayed 0.5 s after approximately 0.5 seconds from $e(k)$ to classify the "moving" state. At the starting points of "absence," $\hat{e}(k)$ is delayed about 3 seconds to classify the "absence" state.

B. Classification Results

Table II shows the classification result of our method. Correct classification results, *TR*, *TM* and *TA* report 0.31, 0.31 and 0.30, respectively, and are counted more often than any other classification results. For the incorrect classification results, *FM*2 and *FA*2 both reported 0.3. Table III shows the classification results of using a HMM whose state transition has no restraints. Each type of the classification results is reported about the same value, 0.09–0.16 and 0.34 accuracy. Moreover, when only $OS(k)$ is used for HMM, the presence/absence is classified as shown in Table IV. Accuracies of the presence/ absence and "moving"/"resting" classifications are 0.97 and 0.79, respectively. When only $OR(k)$ is used for HMM, the presence/absence is classified as shown in Table V. Accuracies of the presence/absence and "moving"/"resting" classifications are 0.81 and 0.95, respectively.

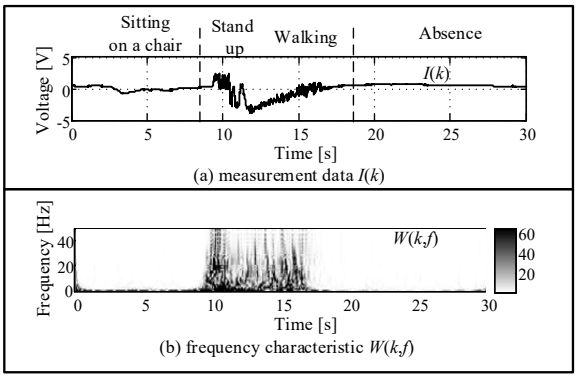

Fig. 3 Example of $I(k)$ and $W(k,f)$

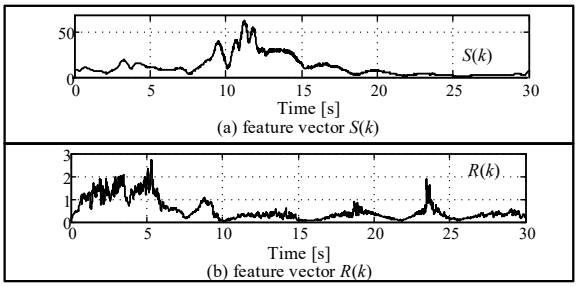

Fig. 4 Example of $S(k)$ and $R(k)$

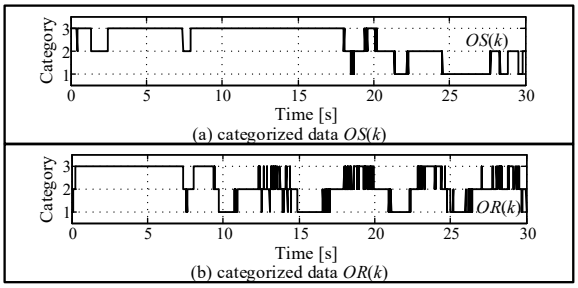

Fig. 5 Example of $OS(k)$ and $OR(k)$

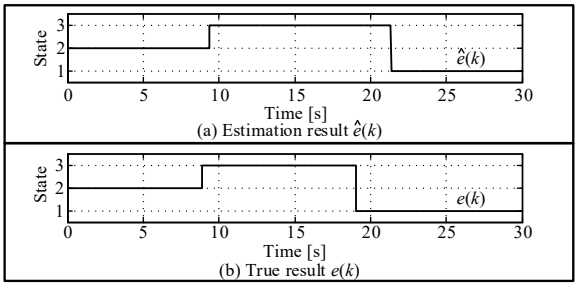

Fig. 6 Example of estimation result, $\hat{e}(k)$ and true result, $e(k)$

TABLE II
CLASSIFICATION RESULT OF OUR METHOD

		True state		
		Resting	Moving	Absence
Classified state	Resting	0.31	0.01	0
	Moving	0.01	0.31	0.03
	Absence	0.01	0.03	0.30

TABLE III
CLASSIFICATION RESULT OF USING HMM WITH NO RESTRAINT OF STATE TRANSITION

		True state		
		Resting	Moving	Absence
Classified state	Resting	0.10	0.09	0.15
	Moving	0.09	0.16	0.09
	Absence	0.13	0.10	0.09

TABLE IV
CLASSIFICATION RESULT OF USING ONLY $OS(K)$

		True state		
		Resting	Moving	Absence
Classified state	Resting	0.22	0.04	0
	Moving	0.10	0.30	0.07
	Absence	0	0.01	0.26

Gray position represents correct cases if presence/absence is classified.

TABLE V
CLASSIFICATION RESULT OF USING ONLY $OR(K)$

		True state		
		Resting	Moving	Absence
Classified state	Resting	0.31	0.01	0
	Moving	0.02	0.24	0.05
	Absence	0.00	0.10	0.28

Gray position represents correct cases if presence/absence is classified.

V. DISCUSSIONS

From Table IV, $OS(k)$ is shown useful for the classification of a human's presence/absence. Additionally, from Table V, $OR(k)$ is shown useful for the classification of the "resting" and "moving" states. Therefore, when using both $OS(k)$ and $OR(k)$, the three states, "resting", "moving" and "absence", are classified more accurately. We conclude that because the focus was on the respirational frequency band, accurate classifications can be gained. The summation of amplitude between a human's frequency band, $S(k)$, becomes the characteristic of a human's presence/absence. Moreover, $R(k)$, the amplitude ratio of a human's frequency band and other motions' frequency bands, becomes the characteristic of a human's "resting"/"moving." In addition, state transition restraint plays an important role in classifying the three states. In real situations, two transitions: "absence" to "resting," and "resting" to "absence," could not be realized. Our model eliminates the latter restraint as it is capable of classifying the transitions of three states, from "resting" to "absence," the "moving" state.

Future work will include building a model of the state transition from "moving" to "absence" state. Moreover, combined with our previous method [11], the validation for wandering detection is required.

VI. CONCLUSIONS

In this paper, we classified a subject's state as "absence," "resting," and "moving" by developing a transition model for these three states. Our method can classify the states with 0.92 accuracy. Two types of feature vectors are utilized from the respiration frequency bands. The first feature vector, which is useful in distinguishing a human's presence from absence, is obtained from the summation of amplitudes in the respirational frequency band. Moreover, the second feature vector, which is useful for classifying a human's "moving" and "resting" states, is obtained from the amplitudes ratio of the respirational frequency bands and other frequency bands. For our modeling, we used an ergodic topology model with the restraint that no transition occurs between the "resting" and "moving" states.

For future work, the transition from "moving" to "absence" should be taken into account. Moreover, in this experiment, we used relatively young subjects and measured the data in our laboratory. To better portray real situations, measurements should be performed on elderly subjects, particularly ones with dementia, in their homes.

ACKNOWLEDGMENT

A part of this work was supported by JSPS KAKENHI Grant Number 16K16392.

REFERENCES

[1] "World Population Ageing," United Nations, Department of Economic and Social Affairs, Population Division, New York, USA, ST/ESA/SER.A/390, p. 2 2015.
[2] J. Heinik: "Families' and professional caregivers' R. Laudau, G.K. Auslander, S. Werner, N. Shoval, and views of using advanced technology to track people with dementia", Psychogeriatrics, Vol. 1, No. 2, pp.20-35, 2010.
[3] G. Cipriani, C. Lucetti, A. Nuti, and S. Danti, "Wandering and Dementia", Psychogeriatrics, Vol.14, No. 2, pp. 135-142, 2014
[4] A. Solanas, E. Batista, F. Borras, A. M. Balleste, and C. Patsakis, "Wandering analysis with mobile phones: On the relation between randomness and wandering", International Conference on Pervasive and Embedded Computing and Communication Systems, pp. 168-173, 2015
[5] C.-Y. Ko, F.-Y. Leu, and I.-T. Lin, "A Wandering Path Tracking and Fall Detection System for People with Dementia", Broadband and Wireless Computing, Communication and Applications, pp.306-311, 2014.DOI:10.1109/BWCCA.2014.127
[6] S. Elloumi, S. cosar, G. Pusiol, F. Bremond and M. Thonnat, "Unsupervised discovery of human activities from long-time videos", Institution of Engineering and Technology, vol. 9, no. 4, pp. 522-530, 2015.
[7] J. Lu, T. Zhang, F. Hu & Q. Hao, "Preprocessing Design in Pyroelectric Infrared Sensor-Based Human-Tracking System: On Sensor Selection and Calibration", IEEE Transactions on Systems, Man, and Cybernetics: Systems, vol. 47, no. 2, pp. 263-275, 2017.
[8] R. Ma, F. Hu, and Q. Hao, "Active Compressive Sensing via Pyroelectric Infrared Sensor for Human Situation Recognition", IEEE Transactions on Man, and Cybernetics: Systems, DOI: 10.1109/TSMC.2016.2578465, 2017.
[9] M. Sekine, K. Maeno, and T. Kamakura, "Human Detection Algorithm for Doppler Radar Using Prediction Error in Autoregressive Model", IEEE International Symposium on Instrumentation and Control Technology, pp. 37–40, 2012.
[10] D. Okuya, M. Hiramoto, and K. Maeno: Human Sensing Technique Using Microwave Doppler Radar Based on Higher-order Local Autocorrelation Features, IEICE Technical Report, Vol. 113, No. 28, pp. 13–18, 2013.
[11] K. Shiba, T. Kaburagi, T. Nakamura, K. Ozaki and Y. Kurihara, "Feature Selection Guideline for Presence/Absence classification Using a Microwave Doppler Sensor" , SICE journal of Control, Measurement, and System Integration, vol. 10, no. 5, pp. 418-425, 2017.

K. Shiba was born in 1994 and received his B. E. degree in industrial and system engineering from Aoyama Gakuin University in 2016. His current interest is bio-sensing method.

T. Kaburagi was born in 1980. He received his BSEE, ME, and Ph.D. degrees from Waseda University, Japan in 2003, 2005, and 2009 respectively.

He is an Assistant Professor at the Department of Industrial and Systems Engineering, Aoyama Gakuin University. His current research interests are time-series data analysis, bioinformatics, and information-efficient text input systems.

Y. Kurihara received his M.E. and Ph.D. degrees from the Hosei University, Tokyo, in 2003 and 2009, respectively.

He joined Hitachi Software Engineering Ltd., in 2003. From 2009 to 2013, he served as an Assistant Professor in the Seikei University. From 2013 to the present, he has been serving as an Associate Professor at the Aoyama Gakuin University. He has published 65 journal papers, 80 proceedings for international conferences, and 4 books. His research interests include system engineering, sensing methods, bio-sensing, and system information engineering. He is a member of the Japanese Society for Medical and Biological Engineering, Instrument and Control Engineers, Electrical Engineers of Japan, and the IEEE.